Biomedicine & Pharmacotherapy 81 (2016) 394–401

Available online at
ScienceDirect
www.sciencedirect.com

Elsevier Masson France
EM|consulte
www.em-consulte.com/en

Targeted nano-delivery of novel omega-3 conjugate against hepatocellular carcinoma: Regulating COX-2/bcl-2 expression in an animal model

Azmat Ali Khan[a,*], Amer M. Alanazi[a], Mumtaz Jabeen[b], Iftekhar Hassan[c], Mashooq Ahmad Bhat[a]

[a] Pharmaceutical Biotechnology Laboratory, Department of Pharmaceutical Chemistry, College of Pharmacy, King Saud University, Riyadh 11451, Saudi Arabia
[b] Section of Genetics, Department of Zoology, Aligarh Muslim University, Aligarh 202002, India
[c] Department of Zoology, College of Science, King Saud University, Riyadh 11451, Saudi Arabia

ARTICLE INFO

Article history:
Received 19 December 2015
Received in revised form 14 April 2016
Accepted 17 April 2016

Keywords:
Linolenic acid
Liver cancer
Nano-formulation
Anticancer agent
Omega-3 conjugate

ABSTRACT

The present approach enumerates the effectiveness of tuftsin tagged nano-liposome for the cytosolic transport of 2,6-di-isopropylphenol-linolenic acid conjugate against liver cancer in mice. Initially, the conjugate in its free form was examined for anticancer potential on HepG2 liver cancer cells. Induction of apoptosis and suppression of migration and adhesion of HepG2 cells confirmed the effectiveness of conjugate as an anticancer agent. After this, role of the conjugate entrapped in a nano-carrier was evaluated in animal model. The nano-formulation comprising of conjugate bearing tuftsin tagged liposome was firsly characterized and then its therapeutic effect was determined. The nano-formulation had 100–130 nm size nanoparticles and showed sustained release of the conjugate in the surrounding milieu. The nano-formulation distinctly reduced the expression of COX-2, an important molecule that is vastly expressed in hepatocellular carcinoma. The utilization of in-house engineered nano-formulation was also successful in significantly up-regulating Bax and down-regulating bcl-2 gene expression eventually helping in better survival of treated mice. Histopathological analysis also revealed positive recovery of the general architecture and the violent death of cancer cells by apoptosis at tumor specific site. The site specific delivery of conjugate entrapped in tuftsin tagged liposomes was highly safe as well as efficaceous. Nano-formulation based approach showed a visible chemotherapeutic effect on liver cancer progression in experimental mice thereby making it a potential candidate for treatment of liver cancer in clinical settings.

1. Introduction

The treatment with anticancer drugs mostly leads to toxic effects because of lack of specificity towards cancer cells [1,2]. Due to poor solubility their long term use also cause non-targeted accumulation, that further complicates the issue [3]. To circumvent these problems, drug conjugates from natural sources are being in use nowadays. A great deal of attention has been devoted to the use of dietary omega fatty acids because of the fact that they inhibit tumor cell proliferation and induce apoptosis [4–7]. Certain fatty acids synergistically help other chemotherapeutic drugs in inhibiting tumorigenesis [8–10]. Among various fatty acids, omega-3 type has been reported to suppress various neoplastic diseases [4–6,11]. Its use in diet decrease the threat of cancer and also increase the bioavailability of the existing drug in a targeted manner.

Considering the anticancer potential of omega (unsaturated) fatty acids, we have previously synthesized series of ester conjugates where various mono- and polyunsaturated fatty acids were coupled with an anesthetic agent, di-isopropylphenol [5–7,12]. Our preliminary trials on these conjugates have shown effective killing of cancer cells *in-vitro* through the induction of various apoptotic factors [6,7]. Linolenic acid just like other dietary omega 3 s has been shown to possess anticancer activities [13,14]. It also has anti-oxidative and anti-apoptotic properties [15]. Therefore, the present study was envisaged to establish the

* Corresponding author.
E-mail address: azmatbiotech@gmail.com (A.A. Khan).

http://dx.doi.org/10.1016/j.biopha.2016.04.033
0753-3322/

anticancer effect of novel linolenic acid conjugate on liver cancer cells in-vitro and through conjugate entrapped in the delivery vehicle in animal models.

Liposomes are clinically approved biocompatible material that encapsulate both hydrophobic and hydrophilic drug and demonstrate safe delivery with low toxicity. They are able to control the bio-distribution by altering the size, surface charge, composition and other physical characteristics [18,19]. Because of these advantages, use of liposomes promote anti-tumor potential in comparison with the free drug and other therapeutic procedures. Various conjugate bearing liposomal formulations have been used for the cytosolic delivery of antibiotics and anticancer drugs [18,20,21]. Likewise, tuftsin, a naturally occurring tetrapeptide, have been reported as an anticancer agent in animal model [16]. Co-administration of tuftsin enhance the anticancer efficacy of commercially available drugs and are also able to activate the tumoricidal macrophages that can engulf and suppress the various kind of malignant cells [17].

In the current study, the chemotherapeutic action of the conjugate (2,6-di-isopropylphenol-linolenic acid) entrapped in tuftsin tagged liposomes against the treatment of diethyl nitrosoamine (DEN) induced liver cancer in murine experimental model was assessed. The efficacy of the nano-formulation was ascertained in the management of liver cancer in Swiss albino mice on the basis of regression, survival, histopathology as well as the expression of COX-2, bcl-2 and Bax in the treated animals.

2. Materials and methods

2.1. Materials

All the reagents used were of analytical grade with highest purity. Polyvenylidene difuoride [PVDF] membranes and 0.22 μm size sterile filters were purchased from Millipore (Germany). Diethylnitrosoamine (DEN), propofol, linolenic acid and tuftsin were obtained from Sigma Aldrich (St. Louis, MO, USA). Tuftsin was modified by coupling a hydrocarbon fatty acyl residue to the C-terminus through an ethylenediamine spacer arm (Thr-Lys-Pro-Arg-NH-$(CH_2)_2$-NH-CO-$C_{15}H_{31}$), according to the published protocol that permits almost quantitative incorporation into liposomes [22]. Cell migration and adhesion kits were obtained from Cell Biolabs, Inc. Vybrant Apoptosis Assay Kit #2 was procured from Molecular Probe (Eugene, Oregon).

Anti-COX-2, Anti-bcl-2, Anti-Bax antibody and non fat dry milk were procured from BD Biosciences (San Diego, CA). Rabbit anti-mouse HRP tagged secondary antibody was purchased from Amersham and monoclonal anti-GAPDH was purchased from Sigma Aldrich (St. Louis, MO, USA). Chemiluminescence detection kit was brought from Bio Rad Laboratories, Inc. (CA, USA).

2.2. Assessment of anticancer potential of conjugate on HepG2 cells

2.2.1. Measurement of cancer cell migration and adhesion

Assay for migration and adhesion was performed with cytoselect 24-well cell migration and cell adhesion kits as per Khan et al. [6] protocol. For quantitative analysis, three concentrations viz. 5 μM, 15 μM and 25 μM of the conjugate were tested on HepG2 liver cancer cells. Finally after incubation process, the 100 μl of the sample in 96-well plate was read at 560 nm.

2.2.2. Analysis of annexin-V binding by flow cytometry

Annexin-V staining was performed according to the kit's protocol. After treating with 15 μM conjugate for 48 h the HepG2 cells were harvested and incubated with annexin V-FITC and PI. The fluorescence emission of Annexin-V stained cells was measured at 530–575 nm in a flow cytometer (MACSQuant, Germany).

2.3. Preparation of conjugate entrapped liposomes

Tuftsin tagged liposomes were prepared using published methods with slight modifications [23]. The nano-formulation was made by mixing 10:1 ratio of liposomes with conjugate (2,6-di-isopropylphenol-linolenic acid) [7]. The nano-formulation was then reconstituted with phosphate buffered saline (PBS) and centrifuged at 14,000*g* for 5 min. The pellet was washed three times in PBS and then passed through 100 nm polycarbonate filter for 10–12 cycles to get the desired size of nanoparticles.

2.4. Characterization of conjugate entrapped in liposomes

2.4.1. Transmission electron microscopy (TEM)

A drop of nano-formulation (lyophilized and suspended in 20 mM PBS, pH 7.4) was mounted on clear glass stub. The sample was coated with gold-palladium alloy and imaged at an accelerating voltage of 120 kV on a transmission electron microscope (Model HT7700, Hitachi High Technologies, America Inc.).

2.4.2. Nanophox imaging

The 2 mg of nano-formulation in a lyophilized form was suspended in 1 ml of distilled water and a drop of it was analyzed by the Nanophox particle-size analyzer (Sympatec GmbH, Germany).

2.4.3. Entrapment efficiency and zeta-potential

The entrapment efficiency of the conjugate in nano-liposomes was measured by dissolving an aliquot of formulation in chloroform:methanol [1:9 v/v] solution. Isocratic methanol-water (72:28 v/v) was taken as the solvent system. Entrapped amount was calculated from the respective standard curve plotted at λ_{max} = 272 nm. Percent entrapment efficiency (%EE) was calculated as %EE = (amount of conjugate entrapped)/(total amount of conjugate used in the beginning) × 100.

Zeta [ζ]-potential of conjugate entrapped nano-formulation was measured by Zetasizer Nano ZS (Malvern Instrument Limited, UK). For analysis, the nano-formulation was lyophilized and then suspended in phosphate buffer (pH 7.4).

2.4.4. Release kinetics

The nano-formulation [equivalent to 1 mg of conjugate] was dispersed in 1 ml of 20 mM PBS [pH 7.4]. The suspension was kept in an orbital shaking water bath at 120 rpm at 37 °C. Aliquots of the release medium were saved at different time intervals and were read at 272 nm. Release runs were continued for 144 h. The results obtained were the mean values of three independent experiments.

2.5. Assessment of anticancer potential of nano-formulation in mice

2.5.1. Experimental animals

Healthy male Swiss albino mice (20 ± 2 g body weight) were obtained from the animal house facility and housed in propylene cages under standard atmospheric conditions (22 ± 1 °C temperature; 12 h light/12 h dark photoperiod and 50–60% humidity). The care and handling of mice was done regularly with pellet diet and water *ad libitum*.

2.5.2. Induction of liver cancer by DEN

For induction of liver cancer, 2.4 mg/mouse dose of diethylnitrosoamine (DEN) was injected intraperitoneally [24]. During induction period, the mice were quarantined and examined routinely for gross body morphological changes. After 40 days,

occurrence of cancer was established by histopathology and quantitative levels of liver enzymes.

2.5.3. Determination of LD_{50} of conjugate

LD_{50} was determined according to published protocol [25]. Six sets of mice (6 in each set) were treated with the conjugate, intraperitoneally. The mice were monitored for 1 week at different time intervals for toxic symptoms. After which mortality rate was totaled from each set.

2.5.4. Dose of treatment

The mice were taken in four groups comprising of 20 mice per group. The mice of group I was used as healthy control and received no treatment. Group II mice were applied with DEN and served as untreated control. Group III and IV mice were treated subcutaneously with free conjugate and the nano-formulation, respectively. The treatment continued for 10 consecutive days. After resting phase of one month, the mice were euthanized by CO_2 inhalation. Liver was dissected, washed in PBS, snap frozen in liquid nitrogen, and stored at −80 °C.

2.5.5. Histopathological slide preparation

The 10 μM sections were cut from frozen liver using cryostat MEV (SLEE medical GmbH, Germany). Sections were fixed in 10% formalin in saline water. Hematoxylin and eosin (H&E) stained slides were visualized for histopathological changes at 200× magnification under Olympus CLX 41 microscope.

2.5.6. Extraction of nuclear protein

The liver samples were homogenized in lysis buffer comprising of 20% glycerol, 20 mmol/l HEPES, 10 mmol/l NaCl, 1.5 mmol/l MgCl, 0.1% NP40, 0.2 mmol/l EDTA, 1 mmol/l DTT, 1 μg/ml pepstatin A, 1 μg/ml aprotinin, 100 μ/ml phenylmethylsulfonyl fluoride and protease inhibitor cocktail. For lysis to take action the homogenate was kept for 15 min and then centrifuged at 2000 rpm for 5 min the pellet was sonicated in 500 mmol/l NaCl for nuclear lysis and then incubated for 30 min on ice. Finally, the samples were centrifuged at 15,000 rpm for 15 min at 4 °C and supernatant containing the nuclear extract was saved and stored at −80 °C.

2.5.7. Western blotting

Protein concentration of nuclear fractions of liver cancer tissues was estimated by NanoDrop 2000 (Thermo Scientific, USA) using bovine serum albumin as a standard. For Western blotting, equal amount of protein (30 μg each) samples were resolved on polyacrylamide gel electrophoresis [26]. The resolved bands were electro-blotted onto PVDF membranes. The membranes were treated by 5% non-fat dry milk for 1 h to block the non-specific binding proteins. The membranes were probed with specific anti-Bax, anti-COX-2 and anti-bcl-2 antibodies. Immunoblots were incubated with horseradish peroxidase-conjugated anti-mouse IgG secondary antibodies for 1 h and immunoreactive bands were detected by Enhanced chemiluminisence detection system. The intensity of the bands was quantified using UVI Doc software. To quantify equal loading, membranes were probed with GAPDH antibody.

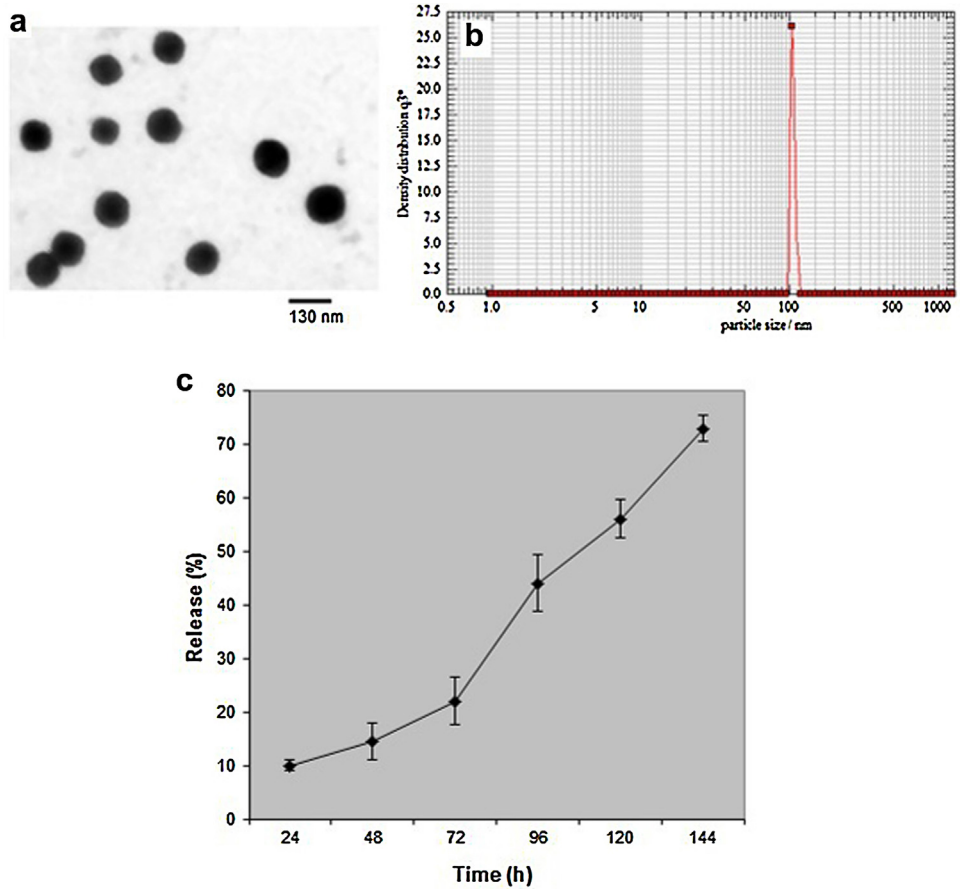

Fig. 1. (a) Transmission electron microscopy image and (b) Corresponding particle size measurement of conjugate bearing tuftsin tagged liposome visualized by the Nanophox particle size analyzer. (c) *In vitro* release of conjugate from tuftsin tagged liposome. Release kinetics graph demonstrates 75% release of conjugate from liposome till 144 h, when formulation was dispersed in 20 mM PBS (pH 7.4) at 37 °C. Data are mean ± SD of three independent experimental values.

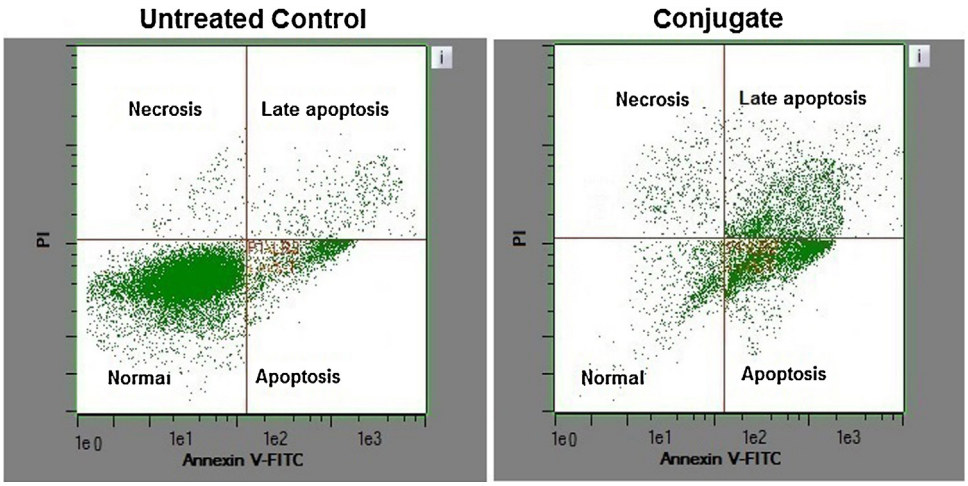

Fig. 2. The apoptotic effect of conjugate using Annexin-V staining against HepG2 cells. Dots represent cells as follows: lower left quadrant, normal cells (Annexin V^-/PI^-); lower right quadrant, apoptotic cells (Annexin V^+/PI^-); upper left quadrant, necrotic cells (Annexin V^-/PI^+), upper right quadrant late apoptotic (Annexin V^+/PI^+). Results are the means ± SD for three experiments with n = 10,000 cells per experiment.

2.6. Statistical analysis

Results were expressed as the mean ± S.D. and were plotted accordingly. Comparative efficacy of the tested formulation was determined by employing standard one-way ANOVA followed by Post hoc analysis done using the Least Statistical Difference (LSD) technique. The Kaplan-Meier method was used to estimate tumor free survival and differences were analyzed by the log-rank test. P values < 0.05 were considered to be statistically significant. The statistical data was evaluated on SPSS v20.0 software.

3. Results

3.1. Effect of conjugate on HepG2 cell migration and adhesion

As shown in Fig. 3a, the conjugate was able to reduce the migration of HepG2 cells in a concentration-dependent pattern. Comparing with the untreated control, the doses of 5 μM, 15 μM and 25 μM significantly inhibited HepG2 migration to about 26% ($P < 0.05$), 30% ($P < 0.05$) and 36% ($P < 0.05$), respectively. Fig. 3b shows the extent of adhesion of HepG2 cells onto a fibronectin surface in the presence of conjugate. The conjugate significantly inhibited cell adhesion by about 32% (5 μM; $P < 0.05$), 35% (15 μM; $P < 0.05$) and 40% (25 μM; $P < 0.05$) in a concentration-dependent manner.

3.2. Annexin V apoptosis detection assay

Among the three concentrations of conjugate, 15 μM showed the optimum effect on HepG2 adhesion and migration. Therefore, only 15 μM concentration of conjugate was used for apoptosis detection. Fig. 2 shows flow cytometric dot plots where annexin V-FITC binding is on the X axis and PI staining is on the Y axis. The dot plots show the response of untreated and conjugate treated HepG2 cells. In the untreated control, the majority of cells were viable (Annexin V^-PI^-) and non-apoptotic. Data from conjugate treated HepG2 cells show a decrease in viable cancer cells and increase in apoptotic cells (Annexin V^+PI^-). After 48 h, the population of apoptotic cells increased from 14.6% in untreated control to 42.2% in conjugate treated group. Increase in the Annexin V^+PI^+ cells due to late apoptosis after 48 h exposure time indicated the death of cells where the apoptosis population increased from 7.4% to 29.1%.

3.3. Charaterization of nanoparticle size by TEM and nanophox

Transmission electron microscopy image represents the mean vesicular size of the conjugate bearing nanoparticles, to be in the range of 100–130 nm (Fig. 1a). Nanoparticles were smooth, spherical and distinct without any clustering, overlapping and assembling. Presence of sharp single distinct peak of approximately 110 ± 10 nm (Fig. 1b) in digital particle size analyser confirmed the size distribution of nanoparticles that was in good agreement with transmission electron microscopy image.

3.4. Entrapment efficiency and zeta-potential

The efficiency of tuftsin-tagged liposome in entrapping a conjugate is determined as the quantity of conjugate inside with respect to the total quantity used during preparation of formulation. The results show an average of 74% entrapment of the conjugate within the tuftsin tagged liposome. Similarly, zeta potential is an important parameter which reveals the surface electronic charge of the nanoparticle when in contact with a liquid aquire. It helps in predicting and controling the stability of the nanoparticle on the basis of net surface charge. The conjugate bearing nanoparticle had the charge of −43.23 ± 1.4 mV.

3.5. Release kinetics assay

The release profile of nano-formulation shows the sustained release pattern over a time period of 144 h. For initial 24 h, only ~10% of the conjugate was released from the nano-formulation. The liposomes were able to release 73% of the conjugate slowly and steadily over an extended time period (Fig. 1c).

3.6. In vivo *anticancer potential of nano-formulation*

3.6.1. LD_{50} of the conjugate

The LD_{50} value of 400 mg/kg body weight was obtained for conjugate upon intraperitoneal application in mice. For treatment,

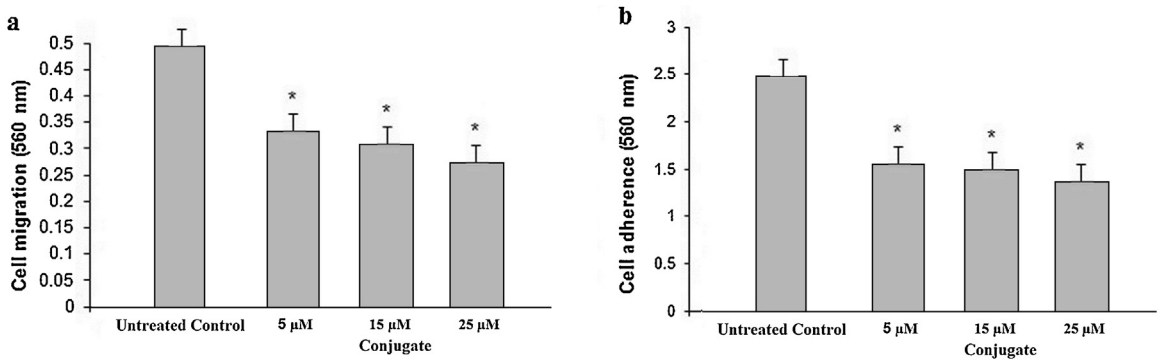

Fig. 3. The inhibitory effect of conjugate on (a) cell migration and (b) cell adherence of HepG2 liver cancer cell lines. Results are the means ± SD for three experiments with $n = 1 \times 10^6$ cells/ml. The level of significance from the control ($P < 0.05$) is indicated with an asterisk.

one-eighth of the lethal dose viz., 50 mg/kg body weight was taken which maintained a 100% survival of mice.

3.6.2. Histopathological changes after treatment with nano-formulation

In the liver of healthy animals, hepatic laminae, sinusoids and hepatocytes were of normal shape. There was no congestion or infiltration, whereas untreated cancerous liver showed loss of normal hepatic structures, including laminae, sinusoids and dilated central vein (Fig. 4a and b, respectively). Nuclear–cytoplasmic dissociation was widespread with focal necrosis. In the conjugate treated Group III, there was the disorganization of laminar structures. However, noticeable regression with marked lytic hepatocellular necrosis, spared oxyphilic hepatocytes with shrunken and dark nuclei (apoptosis) with no congestion was observed (Fig. 4c). Best regression which was visible as maintained hepatic laminar was observed in Group IV mice treated with the nano-formulation. Focal lytic hepatocellular apoptosis was also

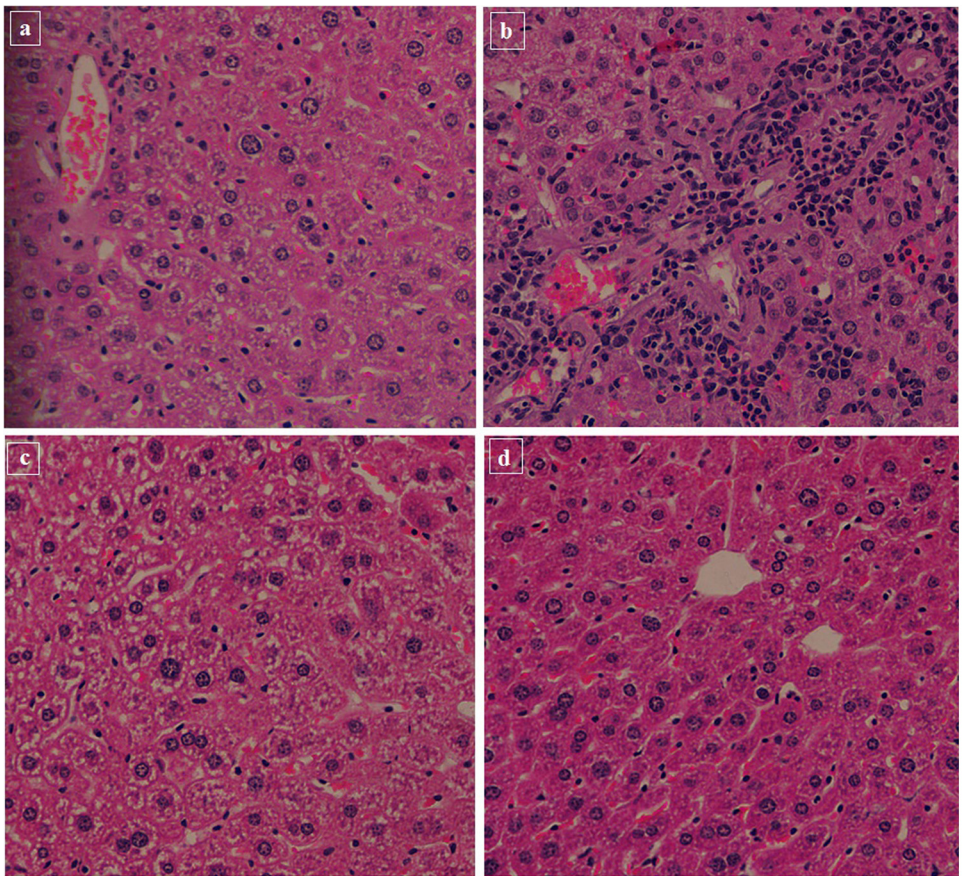

Fig. 4. Histomicrographs of hematoxylin/eosin stained sections of liver tissue of mouse showing (a) Healthy control, (b) Untreated control, (c) conjugate treated and (d) nano-formulation treated. Results are from n = 5 experiments at initiation of therapy.

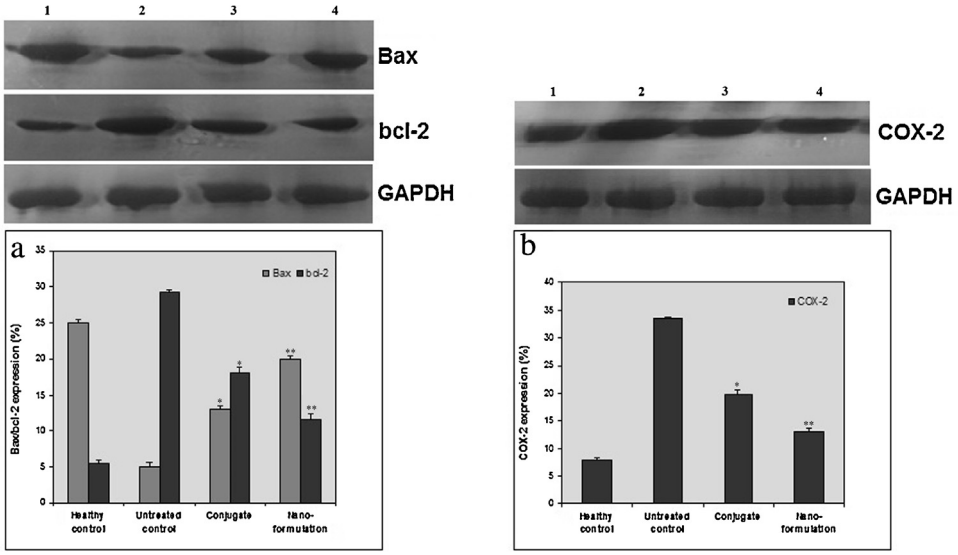

Fig. 5. Immunoblots showing the effect of conjugate bearing tuftsin tagged liposome on the expression of (a) Bax, (b) bcl-2 and (c) COX-2 in treated mice. Lanes: (1) Healthy Control; (2) Untreated Control; (3) Conjugate treated; (4) Nano-formulation treated. Densitograph below shows the relative density of Bax, bcl-2 and COX-2. Results are from n = 5 experiments at initiation of therapy. The level of significance is indicated with an asterisk (Nano-formulation versus untreated control $P < 0.001$, Conjugate versus untreated control $P < 0.01$).

present. No congestion and obvious infiltration with a moderate increase in the Kupffer cell was also vizualized (Fig. 4d).

3.6.3. Expression of apoptotic proteins

The effect of nano-formulation on expression of three major apoptosis-regulating proteins was vizualized employing Western blotting. As seen in Fig. 5a, treatment with the nano-formulation (Group IV) significantly up-regulated the expression of Bax to about 20% ($P < 0.001$) in comparison with DEN exposed untreated mice (Group II). Treatment with the conjugate also increased the Bax expression to 13.2% in relation with untreated mice ($P < 0.01$) (Fig. 5a).

Up-regulation of COX-2 (33.1%) and bcl-2 (28.7%) were recorded in animals exposed to DEN (Fig. 5b and a, respectively; lane 2). In mice treated with the nano-formulation (Group IV), expression levels of COX-2 and bcl-2 were significantly down-regulated to 13.4% ($P < 0.001$) and 11.2% ($P < 0.001$), respectively; in comparison with those observed in Group II mice. Similarly, free conjugate reduced the expression of protein COX-2 (18.5%) and bcl-2 (17.2%) significantly ($P < 0.01$) with respect to Group II mice (Fig. 5b and a, respectively).

3.7. Survival studies

Fig. 6 shows the survivability of cancerous mice treated with the nano-formulation at different time period. In 60 days duration, mice treated with nano-formulation showed significant survival rate of 80% ($P < 0.001$) in comparison with untreated mice. Treatment with free conjugate resulted in 60% survival ($P < 0.01$) whereas there was 0% survival after 30 days of post-treatment in untreated mice (Fig. 6).

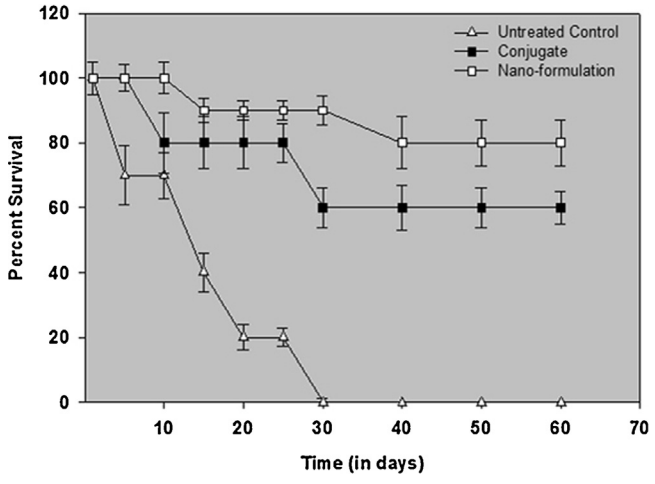

Fig. 6. Effect of nano-formulation on the survival of treated mice. The data was presented as mean ± SD (n = 10 at initiation of therapy). The curve shows the efficacy of nano-formulation in terms of percent survival at different time points post-treatment. The level of significance is indicated with an asterisk (Nano-formulation versus untreated control $P < 0.001$, Conjugate versus untreated control $P < 0.01$).

4. Discussion

Various natural and synthetic compounds have shown their anticancer efficacy *in vitro* and *in vivo* and have been designated as cancer chemopreventive agents [27]. The effectiveness of conjugated fatty acids makes them a potential candidate in cancer treatment and prevention [4,5,28,29]. As of now, anticancer activity of linolenic acid-diisopropylphenol conjugate has not been reported in cancer cell lines and no evaluation has been performed along with the curative potency of its liposomized form in animal models. In the present study, linolenic acid conjugate was tested initially for its ability to induce apoptosis and to halt cell migration and adhesion against HepG2 liver cancer cell line. Results proved the anticancer potential of the conjugate that caused cell death by apoptosis and inhibited cancer cell migration and adhesion (Figs. 2–3).

Regardless of the anticancer potential of conjugates, the reduced uptake and retention in tumor cells pose the major hinderance in successfully using these drug conjugates. Modification of poor pharmaco-kinetics of the drug and its controlled release over target specific tumor can be accomplished employing the delivery vehicle. Several studies have shown the potential use of liposomes as drug delivery vehicle in transporting drug

specifically to the target site in liver cancer [30–32]. Moreover, tuftsin is used as an immunomodulator which enhances the immunity of the host and prevent the growth of cancer cells as well as oxidative stress [33,34]. In the present study, tuftsin tagged liposomes were used for targeted delivery of entrapped conjugate on induced liver cancer in mice. The nano-formulation had all the features of a well-formed nanoparticle. They were of mean size of 100–130 nm (Fig. 1) with a good entrapment efficiency and zeta-potential. The liposomes were also able to release the entrapped conjugate in a slow and sustained manner, thereby resulting in improved bioavailability and efficacy of the conjugate.

Tumor cells have been reported to possess deregulated apoptotic machinery [35]. Many antitumor therapies depend on regulating the disturbed apoptosis in cancerous cells. Several anticancer agents stimulate apoptosis in tumor cells [36]. Considering this, we also evaluated the role of conjugate entrapped in nano-formulation in modulation of apoptotic factors viz., COX-2, bcl-2 and Bax *in vivo*. Several lines of evidence suggest that signaling of COX-2 is associated with carcinogenesis. Substantial *in vitro* and *in vivo* studies have shown the role of COX-2 inhibitors in prevention of hepatocarcinogenesis [37]. In humans, high COX-2 levels are recorded in early stages of hepatocellular carcinoma that are down-regulated in advanced stages [38]. COX-2 derived products are directly involve in inducing bcl-2 expression and inhibition of apoptosis [39]. Bcl-2 plays an important role in progression of cancer cells from an accumulation of genetic alterations, which are critical events in carcinogenesis. This bcl-2 gene reduces the release of cytochrome *c* and is reported to be involved in malignancies and considered a central component in governing cell death via mitochondrial pathways [40]. In response to carcinogenic stimuli in cells, the bcl-2 levels rise and triggers to cancer pathogenesis and may be involved in resistance to cancer treatment [41]. Results of immunoblots (Fig. 5) showed down-regulation of COX-2/bcl-2 and significantly up-regulation of Bax expression in cancer treated mice. This clearly indicates that nano-formulation regulated the expression of bcl-2/Bax by releasing the cytochrome *c* and abolished the neoplastic changes induced by diethylnitrosoamine. Histopathological analysis also revealed the best outcomes of treatment with nano-formulation where regression, prominent recovery and sustenance of the general architecture of hepatic tissue was observed. Necrosis and apoptosis was also visualized in a few areas post-treatment (Fig. 4). Survival data showed a clear cut increase in the chemotherapeutic efficacy of nano-formulation over its free form. The higher survival rate of cancer mice for over 60 days time period was observed upon treatment with liposomal nano-formulation (Fig. 6). The increased efficacy of the nano-formulation could be attributed to the fact that slow release of conjugate from tuftsin tagged liposomes resulted in its better accumulation at the targeted site in treated mice [20,21]. This clearly suggests that entrapment of the conjugate in tuftsin tagged liposomes offers an effective alternative to increase the anticancer potential of conjugate in cancer therapy.

5. Conclusions

The conjugate entrapped in tuftsin tagged liposome showed therapeutic effect and was able to inhibit pro/anti-apoptotic molecules. The developed nano-formulation had all the necessary properties of a nanoparticle as revealed by size, surface charge, stability and sustained release pattern. It not only provided strong inhibition of liver cancer, but also offered tergeted delivery and reduced cytotoxicity to the normal cell populations. The positive effect of nano-formulation on COX-2 and bcl-2 inhibitors and Bax activator significantly reduced the growth of liver cancer *in vivo* by inducing apoptosis. The preliminary study, therefore, shows that the nano-formulation based therapeutic approach is an efficient way of treating liver cancer and can be utilized in clinical settings.

Conflict of interest

The authors declare that they have no conflict of interest.

Acknowledgements

The authors would like to extend their sincere appreciation to the Deanship of Scientific Research at King Saud University for funding of this research through the Research Group Project No. RGP-212.

References

[1] C.R. Miller, H.L. McLeod, Pharmacogenomics of cancer chemotherapy-induced toxicity, J. Support. Oncol. 5 (1) (2007) 9–14.
[2] S.E. James, H. Burden, R. Burgess, Y. Xie, T. Yang, S.M. Massa, F.M. Longo, Q. Lu, Anti-cancer drug induced neurotoxicity and identification of Rho pathway signaling modulators as potential neuroprotectants, Neurotoxicology 29 (4) (2008) 605–612.
[3] E. Merisko-Liversidge, G.G. Liversidge, E.R. Cooper, Nanosizing: a formulation approach for poorly-water-soluble compounds, Eur. J. Pharm. Sci. 18 (2003) 113–120.
[4] R.A. Siddiqui, M. Zerouga, M. Wu, A. Castillo, K. Harvey, G.P. Zaloga, W. Stillwell, Anticancer properties of propofol-docosahexaenoate and propofol-eicosapentaenoate on breast cancer cells, Breast Cancer Res. 7 (2005) R645–R654.
[5] A.A. Khan, M. Alam, S. Tufail, J. Mustafa, M. Owais, Synthesis and characterization of novel PUFA esters exhibiting potential anticancer activities: an *in vitro* study, Eur. J. Med. Chem. 46 (2011) 4878–4886.
[6] A.A. Khan, A. Husain, M. Jabeen, J. Mustafa, M. Owais, Synthesis and characterization of novel n-9 fatty acid conjugates possessing antineoplastic properties, Lipids 47 (2012) 973–986.
[7] A.A. Khan, M. Jabeen, A.A. Khan, M. Owais, Anticancer efficacy of a novel propofol-linoleic acid-loaded escheriosomal formulation against murine hepatocellular carcinoma, Nanomed. (Lond.) 8 (2013) 1281–1294.
[8] A.M. Yvon, P. Wadsworth, M.A. Jordan, Taxol suppresses dynamics of individual microtubules in living human tumor cells, Mol. Biol. Cell 10 (1999) 947.
[9] J.A. Menendez, L. Vellon, R. Colomer, R. Lupu, Oleic acid, the main monounsaturated fatty acid of olive oil, suppresses Her-2/neu (erbB-2) expression and synergistically enhances the growth inhibitory effects of trastuzumab (Herceptin) in breast cancer cells with Her-2/neu oncogene amplification, Ann. Oncol. 16 (2005) 359–371.
[10] M. Jabeen, A.M. Alanazi, I. Hasan, M. Afzal, A.A. Khan, Antigenotoxic and antioxidative effects of novel anticancer conjugate on doxorubicin induced toxicity in mice, Latin Am. J. Pharm. 34 (1) (2015) 101–108.
[11] A.A. Khan, A.M. Alanazi, M. Jabeen, A. Chauhan, A.S. Abdelhameed, Design, synthesis and in vitro anticancer evaluation of a stearic acid-based ester conjugate, Anticancer Res. 33 (6) (2013) 2517–2524.
[12] A.M. Alanazi, A.A. Khan, J. Mustafa, M.K. Parvez, A.S. El-Azab, A.S. Abdelhameed, Characterization and anticancer potential of newly synthesized propofol conjugates, Asian J. Chem. 26 (9) (2014) 2773–2780.
[13] U.N. Das, Tumoricidal and anti-angiogenic actions of gamma-linolenic acid and its derivatives, Curr. Pharm. Biotech. 7 (2006) 457–466.
[14] U.N. Das, N. Madhavi, Effect of polyunsaturated fatty acids on drug-sensitive and resistant tumor cells *in vitro*, Lipids Health Dis. 10 (2011) 159.
[15] S.K. Oh, K.H. Yun, N.J. Yoo, N.H. Kim, M.S. Kim, B.R. Park, J.W. Jeong, Cardioprotective effects of alpha-lipoic acid on myocardial reperfusion injury: suppression of reactive oxygen species generation and activation of mitogen-activated protein kinase, Korean Circ. J. 39 (2009) 359–366.
[16] K. Nishioka, A.A. Amoscato, G.F. Babcock, Tuftsin: a hormone-like tetrapeptide with antimicrobial and antitumor activities, Life Sci. 28 (1981) 1081–1090.
[17] K. Nishioka, G.F. Babcock, J.H. Phillips, R.A. Banks, A.A. Amoscato, In vivo and in vitro antitumor activities of tuftsin, Ann. N. Y. Acad. Sci. 419 (1983) 234–241.
[18] A. Bhatia, B. Singh, K. Raza, A. Shukla, B. Amarji, O.P. Katare, Tamoxifen-loaded novel liposomal formulations: evaluation of anticancer activity on DMBA-TPA induced mouse skin carcinogenesis, J. Drug Target. 20 (6) (2012) 544–550.
[19] O.P. Katare, K. Raza, B. Singh, S. Dogra, Novel drug delivery systems in topical treatment of psoriasis: rigors and vigors, Indian J. Dermatol. Venereol. Leprol. 76 (2010) 612–621.
[20] G.M.M. El Maghraby, A.C. Williams, B.W. Barry, Skin delivery of 5-fluorouracil from ultradeformable and standard liposomes in vitro, J. Pharm. Pharmacol. 53 (2001) 1069–1077.
[21] J.Y. Fang, C.F. Hung, T.L. Hwang, Y.L. Huang, Physicochemical characteristics and in vivo deposition of liposome-encapsulated tea catechins by topical and intratumor administrations, J. Drug Target. 13 (2005) 19–27.

[22] A. Singhal, A. Bali, R.K. Jain, C.M. Gupta, Specific interactions of liposomes with PMN leukocytes upon incorporating tuftsin in their bilayers, FEBS Lett. 178 (1958) 109–113.
[23] A. Agarwal, H. Kandpal, H.P. Gupta, N.B. Singh, C.M. Gupta, Tuftsin-bearing liposomes as rifampin vehicles in treatment of tuberculosis in mice, Antimicrob. Agents Chemother. (1994) 588–593.
[24] H.C. Pitot, L. Barsness, T. Goldsworthy, T. Kitagawa, Biochemical characterisation of stages of hepatocarcinogenesis after a single dose of diethylnitrosamine, Nature 271 (5644) (1978) 456–458.
[25] A. Al-Ali, A.A. Alkhawajah, M.A. Randhawa, N.A. Shaikh, Oral and intraperitoneal LD50 of thymoquinone, an active principle of *Nigella sativa*, in mice and rats, J. Ayub Med. Coll. 20 (2008) 25–27.
[26] U.K. Laemmli, Cleavage of structural proteins during the assembly of the head of bacteriophage T4, Nature 227 (1970) 680–685.
[27] G.J. Kelloff, J.A. Crowell, V.E. Steele, R.A. Lubet, W.A. Malone, C.W. Boone, L. Kopelovich, E.T. Hawk, R. Lieberman, J.A. Lawrence, I. Ali, J.L. Viner, C.C. Sigman, Progress in cancer chemoprevention: development of diet derived chemoprevention agents, J. Nutr. 130 (2000) 467S–471S.
[28] M.P. Moyer, W.E. Hardman, Cameron I. U.S. Patent Application 2002-102907 200220322, Priority: US 2001-278138, 2003, pp 27.
[29] J.A. Menendez, S. Ropero, R. Lupu, R. Colomer, Omega-6 polyunsaturated fatty acid gamma-linolenic acid (18:3n-6) enhances docetaxel (Taxotere) cytotoxicity in human breast carcinoma cells: relationship to lipid peroxidation and HER-2/neu expression, Oncol. Rep. 11 (2004) 1241–1252.
[30] G. Cevc, Transferosomes, liposomes and other lipid suspensions on the skin: permeation enhancement, vesicle penetration and transdermal drug delivery, Crit. Rev. Ther. Drug Carrier Syst. 13 (1996) 257–388.
[31] G. Betz, A. Aeppli, N. Menshutina, H. Leuenberger, In vivo comparison of various liposome formulations for cosmetic application, Int. J. Pharm. 296 (2005) 44–54.
[32] F. Maestrelli, M.L. Gonzalez-Rodriguez, A.M. Rasco, P. Mura, Preparation and characterization of liposomes encapsulating ketoprofen-cyclodextrin complexes for transdermal drug delivery, Int. J. Pharm. 298 (2005) 55–67.
[33] A. Knyszynski, B. Gottilieb, M. Fridkin, Inhibition by tuftsin of Rauscher virus leukemia development in mice, J. Nat. Cancer Inst. 71 (1983) 87–90.
[34] R.D. Noyes, G.F. Babcock, K. Nishioka, Antitumor activity of tuftsin on murine melanoma in vivo, Cancer Treat. Rep. 65 (1981) 673–675.
[35] F.H. Igney, P.H. Krammer, Death and anti-death: tumor resistance to apoptosis, Nat. Rev. Cancer 2 (2002) 277–288.
[36] S.Y. Sun, N. Hail Jr., R. Lotan, Apoptosis as a novel target for cancer chemoprevention, J. Natl. Cancer Inst. 96 (2004) 662–672.
[37] M.A. Kern, M.M. Schoneweiss, D. Sahi, M. Bahlo, A.M. Haugg, H.U. Kasper, H.P. Dienes, H. Kaferstein, K. Breuhahn, P. Schirmacher, Cyclooxygenase-2 inhibitors suppress the growth of human hepatocellular carcinoma implants in nude mice, Carcinogen 25 (2004) 1193–1199.
[38] A. Cusimano, D. Fodera, N. Lampiasi, A. Azzolina, M. Notarbartolo, L. Giannitrapani, N. D'Alessandro, G. Montalto, M. Cervello, Prostaglandin E2 receptors and COX enzymes in human hepatocellular carcinoma: role in the regulation of cell growth, Ann. N. Y. Acad. Sci. 1155 (2009) 300–308.
[39] M.M. Zyada, M.E. Grawish, H.M. E.Lsabaa, Predictive value of cyclooxygenase-2 and bcl2 for cervical lymph node metastasis in mucoepidermoid carcinoma, Ann. Diagn. Pathol. 13 (2009) 313–321.
[40] H. Sheng, J. Shao, J.D. Morrow, R.D. Beauchamp, R.N. DuBois, Modulation of apoptosis and bcl2 expression by prostaglandin E2 in human colon cancer cells, Cancer Res. 58 (1998) 362–366.
[41] S. Howard, C. Bittino, S. Brooke, E. Cheng, R.G. Giffard, R. Sapoolsky, Neuroprotective effects of bcl2 overexpression in hippocampal culture: interactions with pathways of oxidative damage, J. NeuroChem. 83 (2002) 914–923.